International Journal of Multiphase Flow 36 (2010) 432–437

Contents lists available at ScienceDirect

International Journal of Multiphase Flow

journal homepage: www.elsevier.com/locate/ijmulflow

Brief Communication

Subgrid scale fluid velocity timescales seen by inertial particles in large-eddy simulation of particle-laden turbulence

Guodong Jin [a], Guo-Wei He [a,*], Lian-Ping Wang [b], Jian Zhang [a]

[a] LNM, Institute of Mechanics, Chinese Academy of Sciences, Beijing 100190, PR China
[b] Department of Mechanical Engineering, University of Delaware, Newark, DE 19716-3140, USA

ARTICLE INFO

Article history:
Received 8 August 2009
Received in revised form 16 November 2009
Accepted 8 December 2009
Available online 16 December 2009

Keywords:
Particle-laden turbulent flows
Large-eddy simulation
Stochastic model
Particle–subgrid scale model
Particle–subgrid scale eddy interaction timescale

1. Introduction

Large-eddy simulation (LES) has emerged as a promising tool for simulating turbulent flows in general and, in recent years, has also been applied to the particle-laden turbulence with some success (Kassinos et al., 2007). The motion of inertial particles is much more complicated than fluid elements, and therefore, LES of turbulent flow laden with inertial particles encounters new challenges. In the conventional LES, only large-scale eddies are explicitly resolved and the effects of unresolved, small or subgrid scale (SGS) eddies on the large-scale eddies are modeled. The SGS turbulent flow field is not available. The effects of SGS turbulent velocity field on particle motion have been studied by Wang and Squires (1996), Armenio et al. (1999), Yamamoto et al. (2001), Shotorban and Mashayek (2006a,b), Fede and Simonin (2006), Berrouk et al. (2007), Bini and Jones (2008), and Pozorski and Apte (2009), amongst others. One contemporary method to include the effects of SGS eddies on inertial particle motions is to introduce a stochastic differential equation (SDE), that is, a Langevin stochastic equation to model the SGS fluid velocity seen by inertial particles (Fede et al., 2006; Shotorban and Mashayek, 2006a; Shotorban and Mashayek, 2006b; Berrouk et al., 2007; Bini and Jones, 2008; Pozorski and Apte, 2009). However, the accuracy of such a Langevin equation model depends primarily on the prescription of the SGS fluid velocity autocorrelation time seen by an inertial particle or the inertial particle–SGS eddy interaction timescale (denoted by δT_{Lp}) and a second model constant in the diffusion term which controls the intensity of the random force received by an inertial particle (denoted by C_0, see Eq. (7)). From the theoretical point of view, δT_{Lp} differs significantly from the Lagrangian fluid velocity correlation time (Reeks, 1977; Wang and Stock, 1993), and this carries the essential nonlinearity in the statistical modeling of particle motion. δT_{Lp} and C_0 may depend on the filter width and particle Stokes number even for a given turbulent flow. In previous studies, δT_{Lp} is modeled either by the fluid SGS Lagrangian timescale (Fede et al., 2006; Shotorban and Mashayek, 2006b; Pozorski and Apte, 2009; Bini and Jones, 2008) or by a simple extension of the timescale obtained from the full flow field (Berrouk et al., 2007).

In this work, we shall study the subtle and non-monotonic dependence of δT_{Lp} on the filter width and particle Stokes number using a flow field obtained from Direct Numerical Simulation (DNS). We then propose an empirical closure model for δT_{Lp}. Finally, the model is validated against LES of particle-laden turbulence in predicting single-particle statistics such as particle kinetic energy. As a first step, we consider the particle motion under the one-way coupling assumption in isotropic turbulent flow and neglect the gravitational settling effect. The one-way coupling assumption is only valid for low particle mass loading.

* Corresponding author. Tel.: +86 10 82543969; fax: +86 10 82543408.
E-mail addresses: hgw@lnm.imech.ac.cn, guoweihe@yahoo.com (G.-W. He).

0301-9322/$ - see front matter
doi:10.1016/j.ijmultiphaseflow.2009.12.005

2. Governing equations

The study is performed in a forced isotropic turbulent flow field in a periodic box of side 2π. Pseudo-spectral method is used to solve both the Navier–Stokes equations in DNS (Wang et al., 2000) and the filtered Navier–Stokes equations in LES (Yang et al., 2008). The locations and velocities of non-settling heavy particles ($\rho_p \gg \rho_f$) are obtained from the equations of motion as

$$\frac{d\boldsymbol{x}_p(t)}{dt} = \boldsymbol{v}_p(t), \tag{1}$$

$$\frac{d\boldsymbol{v}_p(t)}{dt} = \frac{[\boldsymbol{u}(\boldsymbol{x}_p(t),t) - \boldsymbol{v}_p(t)]f}{\tau_p}, \tag{2}$$

where $\boldsymbol{x}_p(t)$ and $\boldsymbol{v}_p(t)$ are the instantaneous position and velocity of a particle, respectively, τ_p is the particle Stokes relaxation time. f is the correction factor for nonlinear drag which depends on the particle Reynolds number, $f(\mathrm{Re}_p) = 1 + 0.15\mathrm{Re}_p^{0.687}$ and $\mathrm{Re}_p = |\boldsymbol{u} - \boldsymbol{v}_p| d_p/\nu$. As a quick estimate, if we assume that the relative velocity in the definition of Re_p is scaled as the root mean square (rms) velocity, $u_{\mathrm{rms}} = 19.32$, and the particle diameter is half of the Kolmogorov length scale, η, $d_p = 0.5\eta = 0.00675$, the fluid kinematical viscosity is $\nu = 0.0488$ in this study, then the Reynolds number based on the rms velocity is $\mathrm{Re}_p = 1.48$. Since the particle Stokes number may be much larger than one in practice, then the correct factor f in Eq. (2) accounts for the nonlinear drag effect. The fluid velocity seen by an inertial particle, $u_i(\mathbf{x}_p(t), t)$, is a sum of the resolved fluid velocity seen by the particle, $\tilde{u}_i(\mathbf{x}_p(t), t)$, and the unresolved fluid velocity seen by the particle, $u_i(\mathbf{x}_p(t), t) - \tilde{u}_i(\mathbf{x}_p(t), t)$. The resolved flow is calculated from the filtered Navier–Stokes equations in LES

$$\frac{\partial \tilde{u}_i}{\partial x_i} = 0,$$

$$\frac{\partial \tilde{u}_i}{\partial t} + \tilde{u}_j \frac{\partial \tilde{u}_i}{\partial x_j} = -\frac{\partial \tilde{p}}{\partial x_i} + \frac{1}{Re} \frac{\partial^2 \tilde{u}_i}{\partial x_j \partial x_j} - \frac{\partial \tau_{ij}}{\partial x_j} + f_i, \tag{3}$$

where $\tau_{ij} = \widetilde{u_i u_j} - \tilde{u}_i \tilde{u}_j$ is the residual stress tensor, f_i is a large-scale random forcing which is non-zero only at low wavenumbers in Fourier space $|\boldsymbol{k}| < \sqrt{8}$ (Wang et al., 2000). $\tilde{u}_i(\mathbf{x}_p(t), t)$ is obtained from the LES flow fields by a six-point Lagrangian interpolation scheme in each direction (Yang et al., 2008). In this study, the Chollet–Lesieur spectral eddy viscosity SGS model is used for the closure of the filtered Navier–Stokes equations (Chollet and Lesieur, 1981; Chollet, 1983)

$$\nu_e(k|k_c) = \nu_e^+(k/k_c)\sqrt{\frac{E(k_c)}{k_c}}, \tag{4}$$

with

$$\nu_e^+(k/k_c) = C_K^{-3/2}[0.441 + 15.2\exp(-3.03k_c/k)], \tag{5}$$

where C_K is the Kolmogorov constant and $C_K = 2.09$ from the compensated energy spectrum $\varepsilon^{-2/3}k^{5/3}E(k)$ in this paper. The value of C_K in our simulation is consistent with that of Kaneda et al. (1999). $E(k_c)$ in Eq. (4) is the value of the energy spectrum function at the cutoff wavenumber k_c and it is dynamically evaluated from the LES fluid field.

Similar to the previous studies (Fede et al., 2006), the full fluid velocity seen by an inertial particle is then modeled using an extended, stochastic Langevin equation as

$$du_i^+ = \{\tilde{u}_i[x_p(t+dt), t+dt] - \tilde{u}_i[x_p(t), t]\} - \frac{1}{\delta T_{Lp}}(u_i^+ - \tilde{u}_i)dt + \left(\frac{4}{3}k_{\mathrm{SGS},p}\frac{dt}{\delta T_{Lp}}\right)^{1/2}\xi, \tag{6}$$

where the superscript + in Eq. (6) denotes the modeled full scale velocity, of which one part is from the resolved velocity in LES, and the other part is from the Langevin equation. The modeled full scale velocity is different from the real full scale velocity from the Navier–Stokes equation in DNS. ξ is a Gaussian random variable of zero mean and unit variance, $k_{\mathrm{SGS},p}$ is the fluid SGS kinetic energy seen by an inertial particle, which may not be equal to the fluid SGS kinetic energy averaged over the whole space, k_{SGS}. An empirical constant is then introduced to related the two:

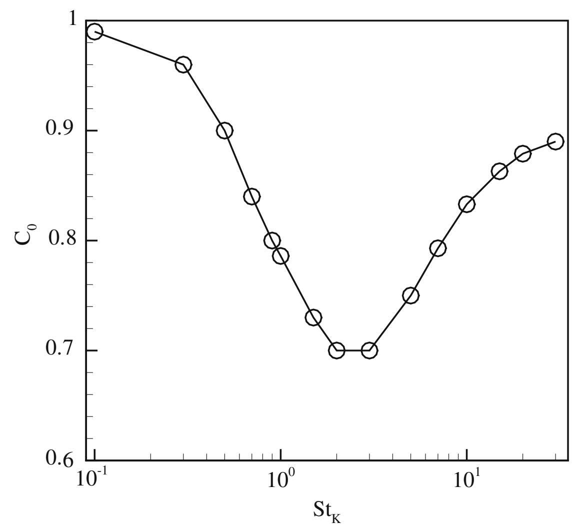

Fig. 1. Variation of C_0 with particle Stokes number, St_K, where C_0 is the ratio of the SGS fluid turbulent kinetic energy seen by inertial particles $k_{\mathrm{SGS},p}$ to the average SGS fluid turbulent kinetic energy averaged over the whole space, k_{SGS}, which is obtained from the energy spectrum of the DNS flow field by $k_{\mathrm{SGS}} = \int_{k_{cf}}^{k_{\max}} E(k)dk$. The cutoff location is at $\eta k_{cf} = 0.135$ and $k_{\max}$ is the maximum wavenumber in DNS.

$$k_{\mathrm{SGS},p} = C_0 k_{\mathrm{SGS}}, \tag{7}$$

where, due to the inertial bias, C_0 could depend on the Stokes number. Using the DNS flow field, we can compute both $k_{\mathrm{SGS},p}$ and k_{SGS} and therefore determine C_0. Fig. 1 shows how C_0 varies with particle Stokes number, St_K, where St_K is defined as $\mathrm{St}_K \equiv \tau_p/\tau_K$ and τ_K is Kolmogorov timescale in DNS flow field, the cutoff location is at $\eta k_{cf} = 0.135$ and k_{cf} is the cutoff wavenumber used in the filtered-DNS. When the Stokes number is very small or very large, particles uniformly distribute in the flow fields, therefore, C_0 tends to be 1. However, when the Stokes number is on the order of 1, particles are found preferentially in the regions of low vorticity and high strain rate, leading to significantly lower SGS turbulent kinetic energy. The feature is consistent with the recent observation by Strutt and Lightstone (2006) who showed that there is a net migration of particles towards regions of low kinetic energy. In their idealized model, the flow is composed of two regions of constant turbulent kinetic energy. They found that there is a higher probability for particles to travel into the low kinetic energy region when compared to the region of high kinetic energy.

The above Langevin equation assumes that the SGS fluid flow is isotropic. It ensures that the Lagrangian SGS fluid velocity time scale δT_{Lp} and the fluid SGS kinetic energy seen by an inertial particle $k_{\mathrm{SGS},p}$ are both consistently realized.

The equation of motion, Eq. (2), is integrated with a fourth-order Adams–Bashforth method for the particle velocity and then a fourth-order Adams–Moulton method for the particle location, Eq. (1). When the particle inertia is negligibly small, Eqs. (1), (2) and (6) together reduce to the governing equation for fluid particles (Gicquel et al., 2002).

The remaining closure problem is how to evaluate δT_{Lp}, a quantity that requires the consideration of the SGS fluid velocity, the particle Stokes number as well as the filter width.

3. Evaluation of δT_{Lp}

The simplest closure assumption used in recent studies (Fede et al., 2006; Shotorban and Mashayek, 2006b; Bini and Jones, 2008; Pozorski and Apte, 2009) states that δT_{Lp} is equal to the SGS fluid velocity autocorrelation time δT_L seen by a fluid element. This is true only in the limit that $\mathrm{St} \ll 1$. Previously, Wang and Stock (1993) showed that the integral timescale T_{Lp} of the fluid velocity seen by an inertial particle can vary from the fluid Lagrangian integral time T_L to the fluid Eulerian one-point integral time T_E as the particle inertia is increased in the full scale velocity field of an isotropic turbulence. Based on the numerical simulations they proposed that

$$\frac{T_{Lp}}{T_E} = 1 - \left(1 - \frac{T_L}{T_E}\right) \frac{1}{(1+\mathrm{St}^*)^{0.4(1+0.01\mathrm{St}^*)}}, \tag{8}$$

where the particle Stokes number is defined as $\mathrm{St}^* = \tau_p / T_E$. It is noted that all the parameters in Eq. (8), T_E, T_L/T_E and St^* are based on the full scale velocity field. Berrouk et al. (2007) extended the Wang–Stock model, Eq. (8), in the context of LES by introducing a model for δT_{Lp} as

$$\delta T_{Lp} = \frac{\delta T_L}{\beta} \left[1 - \frac{(1-\beta)}{(1+\mathrm{St})^{0.4(1+0.01\mathrm{St})}} \right], \tag{9}$$

where St is the particle Stokes number, defined as $\mathrm{St} \equiv \tau_p / \delta T_E$, β is the ratio of δT_L to the fluid Eulerian SGS integral time δT_E. It is important to point out that all the parameters in Eq. (9), δT_E, β and St are based on the subgrid scale velocity field. They further assumed that

$$\beta \equiv \frac{\delta T_L}{\delta T_E} = \frac{T_L}{T_E}. \tag{10}$$

Eq. (10) states that the ratio of δT_L to δT_E in the SGS flow field is equal to the ratio of T_L to T_E in the full scale flow field. We will show later that Eq. (10) does not hold for the SGS velocity field. However, when the correct value of β is used, the extended Wang–Stock model, Eq. (9) , can still be applied to capture approximately the dependence of δT_{Lp} on the Stokes number, see Fig. 5.

To evaluate δT_{Lp}, we make use of the flow field $\boldsymbol{u}(\boldsymbol{x}, t)$ obtained from DNS. The key flow parameters of the DNS flow field at 256^3 grid resolution are: Taylor microscale Reynolds number $\mathrm{Re}_\lambda = 102.1$, Kolmogorov time $\tau_K = 0.0037$, Kolmogorov velocity $v_K = 3.63$, fluid Eulerian integral time $T_E = 0.050$ and fluid Lagrangian integral time $T_L = 0.037$. The filtered velocity $\bar{\boldsymbol{u}}(\boldsymbol{x}, t)$ is calculated by truncating the high-wavenumber Fourier modes above a cutoff wavenumber k_{cf}. The subgrid scale velocity is then

$$\boldsymbol{u}'(\boldsymbol{x}, t) = \boldsymbol{u}(\boldsymbol{x}, t) - \bar{\boldsymbol{u}}(\boldsymbol{x}, t). \tag{11}$$

The cutoff wavenumber k_{cf} is varied to obtain the SGS velocity fields with different filter widths (Fede and Simonin, 2006).

At the limit of a very small Stokes number, an inertial particle behaves as a fluid particle. Therefore, we first study the characteristics of the correlation functions and integral timescales of the full fluid velocity and the SGS fluid velocity. The difference between the Eulerian and Lagrangian correlations of the full or unfiltered fluid velocity field, $R_E(\tau)$ and $R_L(\tau)$, has been discussed in many studies (Kaneda and Gotoh, 1991; Yeung, 2001). The Eulerian fluid velocity temporal correlation can be calculated as

$$R_E(\tau) = \frac{\langle u_i(\boldsymbol{x}_0, t_0) u_i(\boldsymbol{x}_0, t_0 + \tau) \rangle}{\langle u_i(\boldsymbol{x}_0, t_0) u_i(\boldsymbol{x}_0, t_0) \rangle}, \tag{12}$$

and the Eulerian integral timescale is then

$$T_E = \int_0^\infty R_E(\tau) d\tau. \tag{13}$$

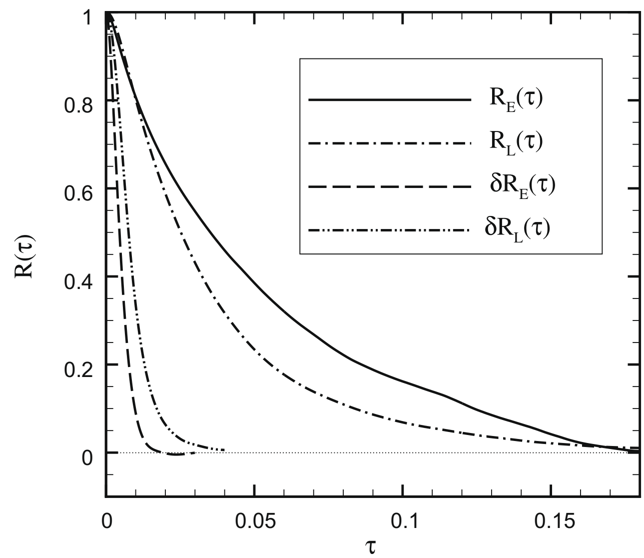

Fig. 2. Eulerian and Lagrangian autocorrelation functions of the full fluid velocity field and the SGS fluid velocity field at $\eta k_{cf} = 0.135$.

The Lagrangian fluid velocity autocorrelation can be calculated as

$$R_L(\tau) = \frac{\langle u_i(\boldsymbol{x}_0, t_0) u_i(\boldsymbol{x}(t_0 + \tau), t_0 + \tau) \rangle}{\langle u_i(\boldsymbol{x}_0, t_0) u_i(\boldsymbol{x}_0, t_0) \rangle}, \tag{14}$$

and the Lagrangian integral timescale is

$$T_L = \int_0^\infty R_L(\tau) d\tau. \tag{15}$$

Fig. 2 shows the Eulerian and Lagrangian autocorrelations for the full velocity field $\boldsymbol{u}(\boldsymbol{x}, t)$. Also shown are the representative Eulerian and Lagrangian velocity autocorrelations for the SGS velocity field $\boldsymbol{u}'(\boldsymbol{x}, t)$ at $\eta k_{cf} = 0.135$. The SGS Eulerian fluid velocity autocorrelation can be calculated as

$$\delta R_E(\tau) = \frac{\langle u_i'(\boldsymbol{x}_0, t_0) u_i'(\boldsymbol{x}_0, t_0 + \tau) \rangle}{\langle u_i'(\boldsymbol{x}_0, t_0) u_i'(\boldsymbol{x}_0, t_0) \rangle}, \tag{16}$$

and the SGS Eulerian integral timescale is

$$\delta T_E = \int_0^\infty \delta R_E(\tau) d\tau. \tag{17}$$

The SGS Lagrangian fluid velocity autocorrelation can be calculated as

$$\delta R_L(\tau) = \frac{\langle u_i'(\boldsymbol{x}_0, t_0) u_i'(\boldsymbol{x}(t_0 + \tau), t_0 + \tau) \rangle}{\langle u_i'(\boldsymbol{x}_0, t_0) u_i'(\boldsymbol{x}_0, t_0) \rangle}, \tag{18}$$

and the SGS Lagrangian integral timescale is

$$\delta T_L = \int_0^\infty \delta R_L(\tau) d\tau. \tag{19}$$

Here, it is important to point out that $\boldsymbol{x}(t_0 + \tau)$ in Eqs. (14) and (18) is the location of a fluid particle based on the full velocity field,

$$\frac{d\boldsymbol{x}(t_0 + \tau)}{d\tau} = \boldsymbol{u}(\boldsymbol{x}(t_0 + \tau), t_0 + \tau). \tag{20}$$

For the full velocity field, $R_E(\tau)$ decays with τ more slowly than $R_L(\tau)$ at large τ. In contrast, for the SGS velocity field, $\delta R_E(\tau)$ drops with τ more quickly than $\delta R_L(\tau)$. These observations imply that $T_E > T_L$ for the full velocity field ($T_L/T_E = 0.74$), while $\delta T_E < \delta T_L$ for the SGS velocity field (in this particular case $\delta T_L/\delta T_E = 1.63$ at

$\eta k_{cf} = 0.135$). The present results are consistent with the previous numerical results showing that T_L/T_E has a typical mean value of 0.78 and is almost independent of Re_λ (Yeung, 2001).

The SGS Eulerian integral timescale, δT_E, can be estimated using the SGS integral length scale, δL, and the rms velocity of the full scale flow field, u_{rms}. This is based on the advection or sweeping effect that the decay of the Eulerian correlation at small-scale is dominated by large-scale sweeping. In the inertial subrange, the SGS integral length scale is $\delta L = 3\pi/10k_{cf}$ and thus the SGS Eulerian integral timescale is (Fede and Simonin, 2006)

$$\delta T_E = \frac{3\pi}{10}\frac{1}{k_{cf}u_{rms}}. \tag{21}$$

For a given turbulent flow field, the SGS Eulerian integral timescale is inversely proportional to the filter width. We plot the variation of δT_E with the filter width in Fig. 3. The circles are the numerical results from Eqs. (12) and (13). The solid line is from Eq. (21). It is observed that the agreement between the numerical results and the sweeping hypothesis is satisfactory. Meanwhile, we numerically calculate the SGS Lagrangian velocity autocorrelation function and SGS Lagrangian integral timescale δT_L using Eqs. (18) and (19), respectively. Fig. 4 shows the SGS integral timescale ratio of δT_L to $\delta T_E, \beta$, from the numerical results. It shows that β is in the range from 1.33 to 2.04 and increases with a scaling of $k_{cf}^{1/3}$ in the inertial subrange. The above conclusion concerning fluid elements alone is very important for developing a model of δT_{Lp}.

We shall now turn to the time scale δT_{Lp} seen by an inertial particle, in particular, the dependence of δT_{Lp} on particle inertia and filter width. δT_{Lp} is obtained by integrating the SGS fluid velocity correlation seen by an inertial particle, $\delta R_{Lp}(\tau)$, with respect to the lag time τ from 0 to ∞. Here, $\delta R_{Lp}(\tau)$ is calculated as

$$\delta R_{Lp}(\tau) = \frac{\langle u_i'(\boldsymbol{x}_p(t_0), t_0)u_i'(\boldsymbol{x}_p((t_0+\tau), t_0+\tau)\rangle}{\langle u_i'(\boldsymbol{x}_p(t_0), t_0)u_i'(\mathbf{x}_p(t_0), t_0)\rangle}, \tag{22}$$

It is important to note that the full velocity field is used here to obtained the particle trajectory $\boldsymbol{x}_p(t)$ from Eqs. (1) and (2). A wide range of Stokes numbers ($St = \tau_p/\delta T_E$) and several filter widths ($\eta k_{cf} = 0.135, 0.216$ and 0.284) were studied. The statistics were computed by tracking 4×10^5 inertial particles. Fig. 5 plots the variation of $\delta T_{Lp}/\delta T_L$ with particle Stokes number St from our DNS results (circle) and a fitted curve (solid line). Several published relations are also shown for comparison (Fede et al., 2006; Shotorban and Mashayek, 2006a; Berrouk et al., 2007).

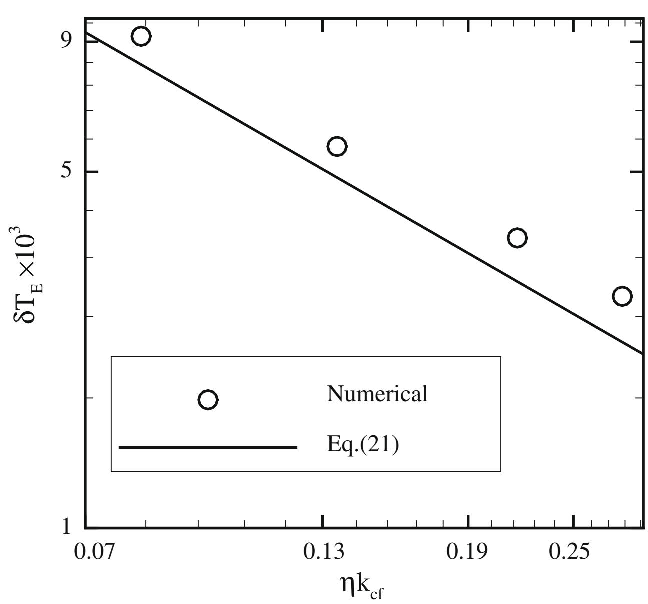

Fig. 3. Variation of the SGS Eulerian integral timescale δT_E with the filter width, ηk_{cf}.

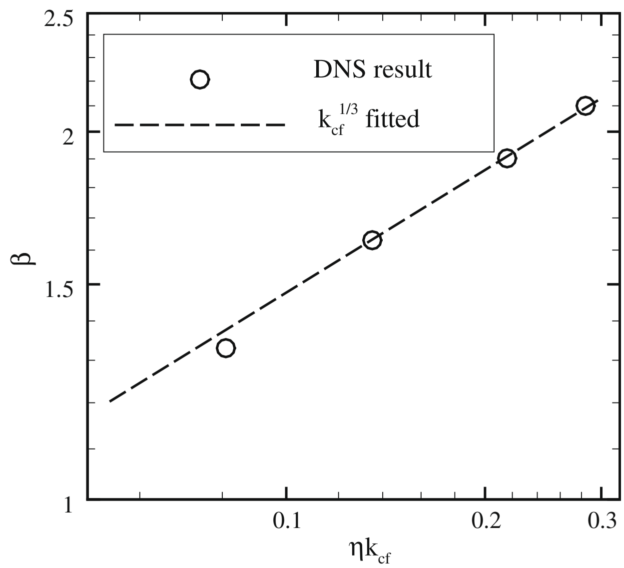

Fig. 4. Dependence of the SGS integral timescale ratio β of δT_L to δT_E on the filter width, ηk_{cf}.

Our DNS results show that for $St < 0.03, \delta T_{Lp} \approx \delta T_L$ or the difference between δT_L and δT_{Lp} is negligible. For the particles with very large inertia, $St \approx 100$ or larger, they do not respond to the SGS eddies, thus $\delta T_{Lp} \to \delta T_E$. For a particle with intermediate inertia, $\delta T_{Lp}/\delta T_L$ varies with St and this variation is *non-monotonic*. The ratio first increases with increasing St, reaches a maximum, and then decreases to approach the limiting value of $\delta T_E/\delta T_L$. That is because, for some range of St, the trajectory of an inertial particle near a SGS eddy tends to deviate from the streamline due to the centrifugal effect or the inertial bias. The inertial particle near a vortex tube experiences a less-curved path along which the SGS fluid velocity does not change so fast and thus the SGS fluid velocity seen by the inertial particle appears to be better correlated. This leads to the ratio $\delta T_{Lp}/\delta T_L$ being larger than one (note that $\delta T_E/\delta T_L < 1$). Such a non-monotonic dependence on Stokes num-

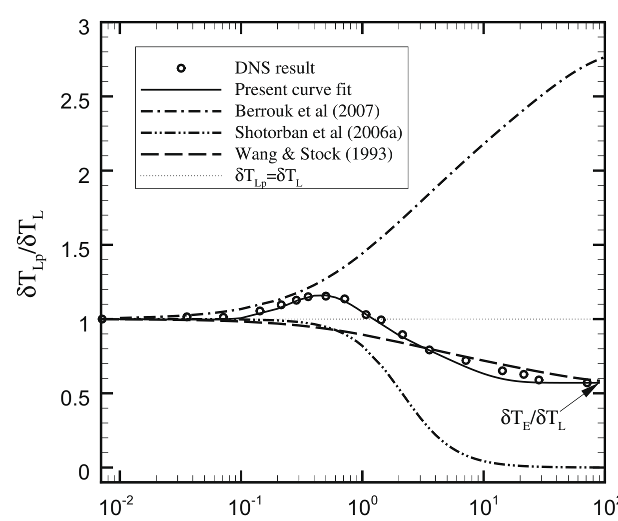

Fig. 5. Variation of $\delta T_{Lp}/\delta T_L$ with particle Stokes number St, where the cutoff location is at $\eta k_{cf} = 0.135, St \equiv \tau_p/\delta T_E$.

ber, St_K, was also seen in the study of Jung et al. (2008) who studied T_{Lp} with unfiltered flow velocity field. A maximum value for $\delta T_{Lp}/\delta T_L$ was observed at $St \sim 0.5$. For larger St, the inertial particle is not very responsive to SGS fluid eddies and therefore, δT_{Lp} gradually approaches δT_E. Our simulation results can be fitted by an empirical curve (solid line in Fig. 5) of the form

$$\frac{\delta T_{Lp}}{\delta T_L}=\frac{1}{\beta}\left\{(0.444-0.7\eta k_{cf})\exp\left\{-\left[\ln\left(\frac{\mathrm{St}}{0.5}\right)\right]^2\right\}+1-(1-\beta)\exp\left(-\frac{\mathrm{St}}{5.15}\right)\right\}, \tag{23}$$

where $\beta = \delta T_L/\delta T_E, k_{cf}$ can be approximately expressed as $k_{cf} = \pi/\triangle$ and $\triangle$ is the length scale of the filter width in physical space (Pope, 2000). This fit was optimized with the results from all three cutoff locations, noting that both δT_L and δT_E also depend on k_{cf}. The above relation captures all the main characteristics of the dependence of δT_{Lp} on St and k_{cf}. It is worth pointing out that the first term in the braces represents that the magnitude of the convexity near $St = 0.5$ depends on the filter width ηk_{cf} when St is small.

Berrouk et al. (2007) used the Wang–Stock model (Wang and Stock, 1993) with $\beta = 0.356$ (dash-dotted line). The model is qualitatively incorrect in the overall trend, implying that their assumption, Eq. (10) should not be used for estimating SGS timescale ratio. However, if we use the the correct value of $\beta = 1.63$ based on the SGS motion when $\eta k_{cf} = 0.135$, the extended Wang–Stock model, Eq. (9), can predict the correct limiting behaviors for $St \to 0$ and $St \to \infty$, and approximately capture the overall trend of the Stokes number dependence (dashed line). As the Wang–Stock model was developed from kinematic random flow fields where the flow dynamics were not considered, the interesting non-monotonic behavior of $\delta T_{Lp}/\delta T_L$ near $St = 0.5$ could not be realized. The dotted line is $\delta T_{Lp} = \delta T_L$ (Fede et al., 2006; Shotorban and Mashayek, 2006b), this assumption is only suitable for very small St (say, $St < 0.05$). Shotorban and Mashayek (2006a) modified the assumption $\delta T_{Lp} = \delta T_L$ by setting $\delta T_{Lp}/\delta T_L = 1/[1 + (\tau_p/\delta T_L)^2]$, their relation is plotted using the dash-dot-dotted line. Their relation would imply that δT_{Lp} monotonically decreases to zero rather than to δT_E, with the increase of St, which is unphysical.

4. Application of δT_{Lp} to the Langevin stochastic model

Finally, we apply the closure model (Eq. (23)) and C_0 shown in Fig. 1 in the Langevin stochastic equation (Eq. (6)) in LES to study the particle kinetic energy.

Fig. 6 compares the ratios of particle kinetic energy to fluid kinetic energy, as a function of Stokes number, St_K, using the present closure. For the range of Stokes numbers studied ($St_K = 0.1 \sim 30$), the conventional LES under-predicts the particle kinetic energy due to the missing of SGS fluid turbulence. However, with the increase of particle Stokes number, the relative difference decreases. This is expected since particles with large Stokes number are less affected by the SGS turbulence. It is observed that the particle SGS Langevin model with our δT_{Lp} formulation greatly improves the accuracy of particle kinetic energy. This result is consistent with the work of (Fede et al., 2006). In Fig. 6, we also include their results. (Fede et al., 2006) performed *a priori* calculations with the filtered DNS flow field and they focused mostly on particles with relaxation time τ_p close to the SGS turbulent timescale of the flow δT_L. The resolution of their DNS flow field is 128^3 and the cutoff location of the filtered-DNS flow field is at $\eta k_{cf} = 0.38$. Their *a priori* calculations also showed a much better prediction when a stochastic Langevin equation is employed. Since we covered a wider range of particle Stokes numbers and used a higher DNS flow Reynolds number, our results show more convincingly that the SGS Langevin model works for small Stokes numbers. The figure also indicates

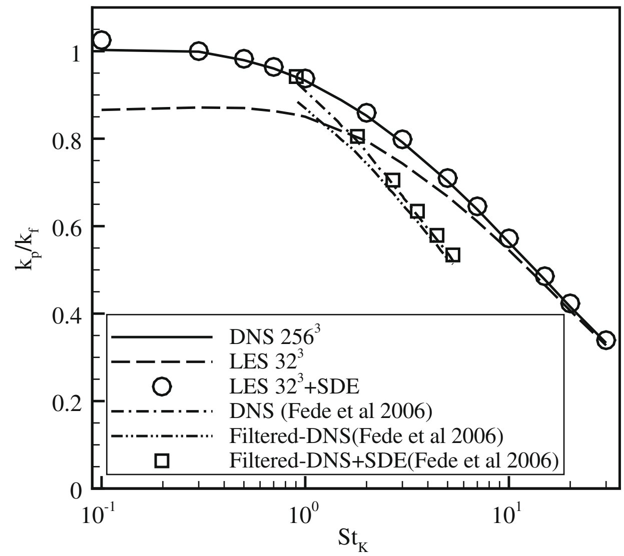

Fig. 6. Comparison of the particle kinetic energy, k_p, with different Stokes numbers, St_K, obtained from the DNS, conventional LES and LES with a subgrid Langevin model, where k_f is the kinetic energy of fluid field. Also shown is the result of (Fede et al., 2006) obtained from the filtered-DNS and a subgrid Langevin model (128^3 DNS and cutoff location $\eta k_{cf} = 0.38$).

that our new closure model for δT_{Lp} led to a better overall prediction.

It should be noted that, under the effect of gravity, a heavy particle moves relatively to the surrounding fluid with a drift velocity, crossing the trajectories of fluid elements and interacting with different small-scale eddies. As a result, we expect that the timescale of the SGS velocity seen by the heavy particle decreases as the settling velocity increases. This is known as the crossing trajectory effect for a heavy particle in turbulent flows, except here in the context of LES the interaction is restricted to SGS turbulent eddies. Furthermore, a related effect is that the timescale in the vertical direction is larger than that in the horizontal direction due to the continuity effect in an incompressible turbulent flow. These effects related to the gravity have been studied by Yudine (1959), Csanady (1963), Reeks (1977), Wells and Stock (1983), and Wang and Stock (1993), amongst others, for the full turbulent flow field. Qualitatively and in the current context of SGS eddies, we expect that the gravity effect is important when the particle settling velocity is comparable to the rms velocity fluctuation of the SGS flow field. The precise dependence of the SGS fluid velocity time scale seen by a particle on the settling velocity requires further investigation.

5. Summary and concluding remarks

In this study, we examined carefully the SGS Lagrangian correlation times seen by both fluid and inertial particles. These SGS Lagrangian statistics show qualitatively different behaviors than the Lagrangian statistics for the full fluid velocity field. For fluid particles, we found that δT_L is larger than δT_E for SGS velocity field, whereas T_L is smaller than T_E for the full velocity field. This suggests that it is important to relate the limiting values of δT_{Lp} to δT_L and δT_E in the SGS flow field, T_L and T_E should not be used in the context of recovering the SGS contributions to particle motion.

Based on the DNS flow field, we computed the SGS fluid velocity correlation time seen by inertial particles, δT_{Lp}, for a wide range of particle Stokes number and several filter widths. It was shown that δT_{Lp} first increases with Stokes number, reaches a peak when St is on the order one, and then decreases with increasing St number. Based on these results, an empirical model for δT_{Lp} is proposed to take into account of the dependence of δT_{Lp} on Stokes number and filter width. Using the Langevin stochastic equation with our new closure model, we demonstrated that the particle kinetic energy can be much better predicted in LES.

We recognize that in some applications, the gravitational settling may also be important. This could complicate the closure of δT_{Lp}. The more difficult problem in LES of particle-laden flows is the prediction of particle-pair statistics, such as the radial distribution function, the pair relative velocity at contact and the collision rate, which are more sensitive to small-scale eddies. These issues remain to be studied.

Acknowledgments

This work was supported by CAS (KJCX2-SW-L08), 973 Program of China (2007CB814800), NSFC (10628206, 10732090, 10702074), the LNM initial funding for young investigators and SRF for ROCS, SEM. G.-D. Jin would like to acknowledge the hospitality received at the Department Mechanical Engineering, University of Delaware during his visit. Part of his visit was supported by the US National Science Foundation under Grant ATM-0527140.

References

Armenio, V., Piomelli, U., Fiorotto, V., 1999. Effect of the subgrid scales on particle motion. Phys. Fluids 11, 3030–3042.

Berrouk, A.S., Laurence, D., Riley, J.J., Stock, D.E., 2007. Stochastic modelling of inertial particle dispersion by subgrid motion for LES of high Reynolds number pipe flow. J. Turbul. 8 (50), 1–20.

Bini, M., Jones, W.P., 2008. Large-eddy simulation of particle-laden turbulent flows. J. Fluid Mech. 614, 207–252.

Chollet, J.-P., 1983. Two-point closures as a subgrid scale modelling for large eddy simulations. In: Durst, F., Launder, B.E. (Eds.), Turbulent Shear Flows, vol. IV. Springer-Verlag, Heidelberg.

Chollet, J.-P., Lesieur, M., 1981. Parameterization of small scales of three-dimensional isotropic turbulence utilizing spectral closure. J. Atmos. Sci. 38, 2747–2757.

Csanady, G.T., 1963. Turbulent diffusion of heavy particles in the atmosphere. J. Atmos. Sci. 20, 201–208.

Fede, P., Simonin, O., 2006. Numerical study of the subgrid fluid turbulence effects on the statistics of heavy colliding particles. Phys. Fluids 18, 045103.

Fede, P., Simonin, O., Villedieu, P., Squires, K.D., 2006. Stochastic modeling of turbulent subgrid fluid velocity along inertial particle trajectories. In: Proceedings of the 2006 CTR Summer Program.

Gicquel, L.Y.M., Givi, P., Jaberi, F.A., Pope, S.B., 2002. Velocity filtered density function for large eddy simulation of turbulent flows. Phys. Fluids 14 (3), 207–252.

Jung, J., Yeo, K., Lee, C., 2008. Behavior of heavy particles in isotropic turbulence. Phys. Rev. E 77, 016307.

Kaneda, Y., Gotoh, K., 1991. Lagrangian velocity autocorrelation in isotropic turbulence. Phys. Fluids A 3, 1924–1933.

Kaneda, Y., Ishihara, T., Gotoh, K., 1999. Taylor expansion in powers of time of Lagrangian and Eulerian two-point two-time velocity correlations in turbulence. Phys. Fluids 11, 2154–2166.

Kassinos, S.C., Langer, C.A., Iaccarino, G., Moin, P., 2007. Complex Effects in Large Eddy Simulations. Springer, Berlin.

Pope, S.B., 2000. Turbulent Flows. Cambridge University Press, Cambridge.

Pozorski, J., Apte, S.V., 2009. Filtered particle tracking in isotropic turbulence and stochastic modeling of subgrid-scale dispersion. Int. J. Multiphase Flow 35, 118–128.

Reeks, M.W., 1977. On the dispersion of small particles suspended in an isotropic turbulent fluid. J. Fluid Mech. 83, 529–546.

Shotorban, B., Mashayek, F., 2006a. On stochastic modeling of heavy particle dispersion in large-eddy simulation of two-phase turbulent flow. In: Balachandar, S., Prosperetti, A. (Eds.), Prodeeding of the IUTAM Symposium on Computational Multiphase Flow. Springer, Netherlands.

Shotorban, B., Mashayek, F., 2006b. A stochastic model for particle motion in large-eddy simulation. J. Turbul. 7 (18), 1–13.

Strutt, H.C., Lightstone, M.F., 2006. Analysis of tracer particle migration in inhomogeneous turbulence. Int. J. Heat Mass Transfer 49, 2557–2566.

Wang, Q., Squires, K.D., 1996. Large eddy simulation of particle-laden turbulent channel flow. Phys. Fluids 8, 1207–1223.

Wang, L.-P., Stock, A.D., 1993. Dispersion of heavy particles by turbulent motion. J. Atmos. Sci. 50 (13), 1897–1913.

Wang, L.-P., Wexler, A.S., Zhou, Y., 2000. Statistical mechanical description and modelling of turbulent collision of inertial particles. J. Fluid Mech. 415, 117–153.

Wells, M.R., Stock, D.E., 1983. The effects of crossing trajectories on the dispersion of particles in a turbulent flow. J. Fluid Mech. 136, 31–62.

Yamamoto, Y., Potthoff, M., Tanaka, T., Kajishima, T., Tsuji, Y., 2001. Large eddy simulation of turbulent gas-particle flow in a vertical channel: effect of considering inter-particle collisions. J. Fluid Mech. 442, 303–334.

Yang, Y., He, G.-W., Wang, L.-P., 2008. Effects of subgrid-scale modeling on Lagrangian statistics in large-eddy simulation. J. Turbul. 9 (8), 1–24.

Yeung, P.K., 2001. Lagrangian characteristics of turbulence and scalar transport in direct numerical simulations. J. Fluid Mech. 427, 241–274.

Yudine, M.I., 1959. Physical considerations on heavy-particle diffusion. Adv. Geophys. 6, 185–191.